Electrochimica Acta 83 (2012) 73–77

Contents lists available at SciVerse ScienceDirect

Electrochimica Acta

journal homepage: www.elsevier.com/locate/electacta

Bionic catalysis of porphyrin for electrochemical detection of nucleic acids

Jie Li, Jianping Lei*, Quanbo Wang, Peng Wang, Huangxian Ju*

State Key Laboratory of Analytical Chemistry for Life Science, Department of Chemistry, Nanjing University, Nanjing 210093, PR China

ARTICLE INFO

Article history:
Received 27 April 2012
Received in revised form 30 July 2012
Accepted 1 August 2012
Available online xxx

Keywords:
Bionic catalysis
Porphyrin
Electrochemistry
DNA
Gold nanoparticles

ABSTRACT

A novel electrochemical strategy was designed for the detection of DNA based on the bionic catalysis of porphyrin. The detection probe was prepared via the assembly of thiolated double strand DNA (dsDNA) with gold nanoparticles (AuNPs), and then interacted with cationic iron (III) meso-tetrakis (*N*-methylphyridinum-4-yl) porphyrin (FeTMPyP) via groove binding along the dsDNA surface. The resulting nanocomplex was characterized with transmission electron microscopy, UV–vis absorption and circular dichroism spectroscopy. The FeTMPyP–DNA–AuNPs probe on gold electrode demonstrated the excellent electrocatalytic behaviors toward the reduction of O_2 due to the largely loading of FeTMPyP and good conductivity. Based on bionic catalysis of porphyrin for the reduction of O_2, the resulting biosensor exhibited a good performance for the detection of DNA with a wide linear range from 1×10^{-12} to 1×10^{-8} mol L^{-1} and detection limit of 2.5×10^{-13} mol L^{-1} at the signal/noise of 3. More importantly, the biosensor presented excellent ability to discriminate the perfectly complementary target and the mismatched stand. This strategy could be conveniently extended for detection of other biomolecules. To the best of our knowledge, this is the first application of bionic catalysis of porphyrin as detection probe and opens new opportunities for sensitive detection of biorecognition events.

1. Introduction

The sensitive detection of DNA sequences has become attractive interesting due to its broad applications in many fields, such as molecular diagnostics, genetics therapy, and early screening of cancers [1–3]. Some signal amplification strategies with the fast catalytic reactions of enzymes have been developed to amplify detection signal for the sensitive detection of DNA [4–11]. However, enzymatic reactions are limited by the mass transfer of substrate molecules toward sensing surfaces due to the blocking effect of large size of enzyme labels [12]. In some cases, poor long-term stability and complex preparation procedures of labeled enzymes make it difficult to obtain highly reproducible assay results. Thus it is urgent to seek a new catalytic label to replace the enzyme, which is required to be high stability, excellent catalysis, low molecular weight, and easy immobilization on a sensing surface.

Porphyrins as an important class of conjugated organic molecules can mimic the active site of many important enzymes [13–16], and can be well used as electron media to catalyze many life-related molecules [17–20]. The controlled organization of porphyrins into highly ordered nanomaterials are expected to have chemical activities significantly different from those of the free porphyrins [21–23], and may lead to applications as electroactive materials. In our previous works, a series of porphyrin functionalized carbon-based nanomaterials were designed to electrocatalyze towards the biological molecules such as peroxyacetic acid, trichloroacetic acid, sulfite and chlorite [24–27]. Nevertheless, to date, there is no report that porphyrins are used as signal labels to replace enzyme labels for highly signal amplification in detection of DNA. Challenges in the development of porphyrin-based detection systems are mainly focused on the organization of the porphyrins on detection probe.

The interactions between porphyrins and DNA have been intensively studied since the pioneering work of Gupta and Pasternack and their coworkers [28–31]. Porphyrins and porphyrin derivatives can associate with DNA in "three-mode binding model": intercalative binding, groove binding or outside binding with self-stacking [29]. In general, free-base porphyrin can intercalate into the GC-rich regions of DNA, while those having axially bound ligands exhibit an outside binding mode [30]. The axially liganded metalloporphyrins, such as Mn^{3+}, Fe^{3+} and Co^{3+} derivatives are able to interact more intimately with the bases of poly(dA–dT) than of poly(dG–dC) [31]. DNA sensing on glassy carbon electrode was developed by using hemin as the electrochemical hybridization label [32]. In this work, a detection probe was prepared by the assembly of cationic iron (III) meso-tetrakis (*N*-methylphyridinum-4-yl) porphyrin (FeTMPyP) with double strand DNA (dsDNA) on gold nanoparticles (AuNPs) via groove binding along the dsDNA surface.

Porphyrin-based nanocomposites can show unique electrochemical properties, and enhanced stability and catalytic rate due to the aggregated structure and the greater surface area for biosensing. Here, a novel electrochemical strategy was designed

* Corresponding authors. Tel.: +86 25 83593593; fax: +86 25 83593593.
E-mail addresses: jpl@nju.edu.cn (J. Lei), hxju@nju.edu.cn (H. Ju).

0013-4686/$ – see front matter © 2012 Elsevier Ltd. All rights reserved.
http://dx.doi.org/10.1016/j.electacta.2012.08.002

for the detection of DNA based on the bionic catalysis of FeTMPyP–DNA–AuNPs probe. The FeTMPyP–DNA–AuNPs probe on gold electrode demonstrated the excellent electrocatalytic behaviors toward the reduction of O_2, since both AuNPs and DNA accelerated the electron transfer between FeTMPyP and the electrode, and increased the amount of adsorbed FeTMPyP. Based on enhanced catalytic current, the designed strategy exhibited a good performance for the detection of DNA, and could be extended to apply in sensitive detection of other biomolecules.

2. Experimental

2.1. Materials and reagents

FeTMPyP is a gift from Kanazawa University (Japan). Chloroauric acid ($HAuCl_4{\cdot}4H_2O$) and trisodium citrate were obtained from Shanghai Reagent Company (Shanghai, China). Tris-(2-carboxyethyl)phosphine hydrochloride (TCEP) and tris(hydroxymethy) aminomethane (Tris) were purchased from Sigma–Aldrich (USA). Phosphate-buffered saline (PBS) was prepared by mixing the stock solutions of NaH_2PO_4 and Na_2HPO_4. Tris–HCl (0.01 mol L^{-1}, pH 7.4) containing 0.001 mol L^{-1} ethylenediaminetetraacetic acid (EDTA) and 0.1 mol L^{-1} NaCl was used as DNA immobilization buffer. Ultrapure water obtained from a Millipore water purification system (≥18 MΩ, Milli-Q, Millipore) was used in all assays. All other reagents were of analytical grade and used as received. The oligonucleotides were purchased from Sangon Biological Engineering Technology & Co. Ltd. (Shanghai, China) and purified using high-performance liquid chromatography. Their sequences are as follows:

Capture 1: 5′HS-TTTTTGTCGAACGGAA-3′;
Capture 2: 5′-AGGTCTCTTCGGTTTTT-SH3′;
Target: 5′-CCGAAGAGACCTTTCCGTTCGAC-3′;
Help 1: 5′HS-$(A)_{25}$-3′;
Help 2: 5′-$(T)_{25}$-3′;
Single-base mismatched: 5′-CCGAAGAGAC**G**TTTCCGTTCGAC-3′;
Three-base mismatched: 5′-CCGA**T**GAGAC**G**TTTCC**C**TTCGAC-3′.

2.2. Apparatus

Electrochemical measurements were performed on a CHI 630D electrochemical analyzer (Chenhua, Shanghai, USA) with a conventional three-electrode system. Gold disk electrode (2 mm in diameter), saturated calomel electrode (SCE) and a Pt electrode were used as the working electrode, reference electrode, and auxiliary electrode, respectively. Differential pulse voltammetry (DPV) was adopted to record the signal due to the high sensitivity and low blank signal. Transmission electron micrographs (TEM) were obtained using a JEM-2100 TEM (JEOL, Japan). The UV–vis spectra were performed with an UV-3600 UV-vis spectrophotometer (Shimadzu, Japan). The circular dichroism (CD) spectra were obtained with J-810/163-900 Circular Dichroism Chiroptical Spectrometer (Jasco, Japan).

2.3. Preparation of detection probe

The colloidal AuNPs were prepared according to the published protocol [33]. Briefly, trisodium citrate (2.5 mL 1%) was added to a boiling solution of $HAuCl_4$ (100 mL 0.01%) accompanied with a color change from pale yellow to deep red. The mixture was allowed to heat another several minutes to ensure complete reduction, and was then slowly cooled to room temperature with stirring to obtain the AuNPs colloid.

The as-prepared AuNPs were further co-functionalized with the dsDNA probe formed via the hybridization between 5′HS-$(A)_{25}$-3′ and 5′-$(T)_{25}$-3′, and the capture 2 [34]. In brief, the thiolated dsDNA probe and the capture 2 were activated by treatment with 1.5 equiv. of TCEP for 1 h at acetate buffer (0.05 mol L^{-1}, pH 5.2) at room temperature. 3 mL of AuNPs (3.94×10^{-9} mol L^{-1}) was incubated with a mixture of dsDNA probe (10 μL, 1×10^{-4} mol L^{-1}) and capture 2 (2 μL, 5×10^{-5} mol L^{-1}) for 16 h at room temperature with gently stirring. Then the mixture was "aged" by gradually addition of 2 mol L^{-1} NaCl and 0.1 M PBS buffer every 8 h until the solution contained 0.1 mol L^{-1} NaCl and 0.01 mol L^{-1} PBS in 24 h at room temperature. The obtained DNA–AuNPs were purified two times by centrifugation (14,000 rpm for 25 min) in order to remove excessive DNA. Then the DNA–AuNPs were dispersed in 0.01 mol L^{-1} PBS (pH 7.4) containing 0.1 mol L^{-1} NaCl to get the DNA–AuNPs solution. Finally, FeTMPyP (100 μL, 3×10^{-4} mol L^{-1}) was added to the as-prepared DNA–AuNPs solution for 0.5 h at room temperature, and obtained the FeTMPyP–DNA–AuNPs probe after washing with Tris–HCl buffer solution twice.

2.4. Fabrication of the biosensor

The fabrication procedure of the biosensor is shown in Scheme 1. Prior to modification, the gold electrode was successively polished to a mirror finish using 1.0 and 0.05 μm alumina slurry (Beuhler). After successive sonication in ethanol and double-distilled water, the electrode was electrochemically polished by cycling in 1 mol L^{-1} H_2SO_4 at a potential scanning between −0.2 V and 1.7 V vs SCE until a reproducible cyclic voltammogram was obtained [35]. Then it was rinsed with doubled-distilled water and allowed to dry at room temperature. 4 μL of thiolated capture 1 DNA (5×10^{-3} mol L^{-1}) was doped to the cleaned electrode. Prior to incubation the disulfide bond, the capture 1 DNA was reduced for 1 h by reaction with 0.01 mol L^{-1} TCEP. After 16 h, the DNA-modified electrodes were thoroughly rinsed with water to remove the weakly adsorbed capture DNA. Then 4 μL target DNA was applied to the electrode and hybridized for 1 h. After raised with doubled-distilled water, 4 μL the as-prepared detection probe was casted to the electrode and reacted for 1 h at room temperature. Finally the electrode surface was washed with water to remove the unbound detection probe for electrochemical measurement.

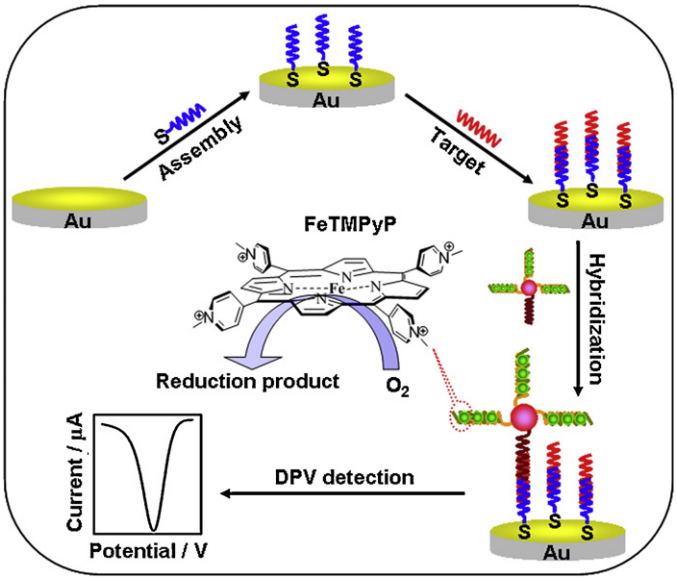

Scheme 1. Schematic representation of assembling processes and detection strategy of the designed biosensor.

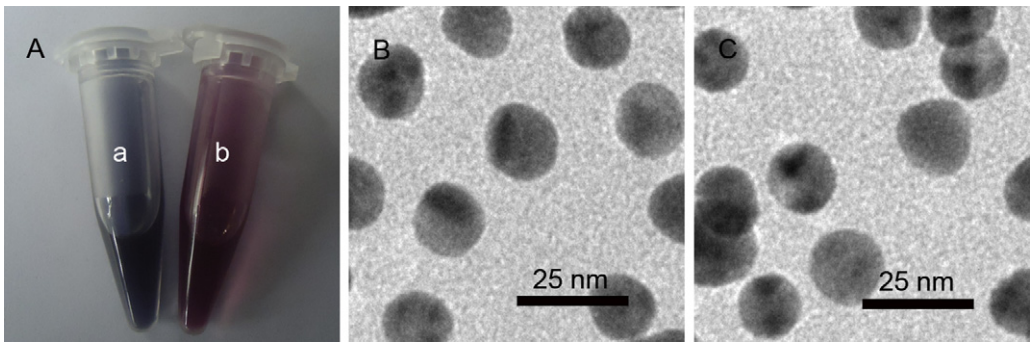

Fig. 1. (A) Photos of AuNPs (a) and DNA–AuNPs (b) in 0.01 mol L^{-1} NaCl, and TEM images of (B) AuNPs and (C) DNA–AuNPs.

3. Results and discussion

3.1. Characterization of the detection probe

Fig. 1 displays the photos of AuNPs and DNA–AuNPs in 0.01 mol L^{-1} NaCl. The freshly prepared AuNPs dispersed well in water and showed a red color. But in certain salt concentration (0.01 mol L^{-1} NaCl), AuNPs were easily aggregated and appeared a purple color (Fig. 1A, photo a) (For interpretation of the references to color in this sentence, the reader is referred to the web version of the article.). After assembling with the thiolated DNA, AuNPs are able to maintain a good dispersion and showed the red color just like the newly prepared AuNPs (Fig. 1A, photo b) (For interpretation of the references to color in this sentence, the reader is referred to the web version of the article.). In order to further identify the good dispersion of the DNA–AuNPs, the TEM images of AuNPs and DNA–AuNPs were investigated in Fig. 1B and C. The prepared AuNPs exhibited a good dispersion with the diameter of around 15 nm (Fig. 1B). After assembling with the thiolated DNA and adding 0.01 mol L^{-1} NaCl, no obvious change can be observed and the particles also showed a good dispersion (Fig. 1C), indicating that the DNA was covalently linked to AuNPs and 'protected' AuNPs from aggregation, which is in accordance with previous report [36].

The resulting DNA–AuNPs could be as platform for the immobilization of porphyrin. In order to prove the binding model between dsDNA and FeTMPyP, the CD spectra were investigated in Fig. 2. In pH 7.4 Tris–HCl buffer, the dsDNA showed a characteristic 'double peak' around 275 nm, indicating that a steady right-handed B-helix dsDNA was formed, providing ideal groove binding sites for FeTMPyP [37]. Furthermore, there is a positive band at 217 nm, which is characteristic for right-handed deoxyadenosine (dA) stacking within the strand (Fig. 2a). Upon addition of FeTMPyP, the band intensity at 217 nm decreased (Fig. 2b), further indicating the groove binding between FeTMPyP and dsDNA, which decreased the interaction among A bases in the original dA stacking [37]. Compared with the fact that there was no obvious CD signature on the solution of FeTMPyP (Fig. 2c), it is confirmed that FeTMPyP was bound to the dsDNA via groove binding model.

In addition, the UV–vis spectra also gave the evidence of the interaction between dsDNA and FeTMPyP. The Soret band of FeTMPyP is 424 nm (Fig. 3, curve b) and exhibited a red-shift of 5 nm upon binding to the dsDNA (Fig. 3, curve a). Obviously the absorption intensity of FeTMPyP–dsDNA reduced greatly compared to the same concentration of FeTMPyP. This result clearly showed that FeTMPyP was self-stacking on the dsDNA and thereby affected the electronic transition capability of FeTMPyP [31,38].

3.2. Electrochemical behaviors of FeTMPyP–DNA–AuNPs modified Au electrode

Cyclic voltammograms of FeTMPyP–DNA–AuNPs modified Au electrode showed the stable and well-defined redox peaks at −0.118 V and −0.163 V vs SCE in N_2-saturated Tris–HCl (Fig. 4, curve a and inset), which should be attributed to the redox couple of $Fe^{(III)}$TMPyP/$Fe^{(II)}$TMPyP. Moreover, the separation of peak potentials of 0.045 V is smaller than 0.058 V for tetraphenylporphyrin/carbon nanotubes modified electrode [39].

Fig. 4 also shows the electrocatalytic response of O_2 at DNA–AuNPs and FeTMPyP–DNA–AuNPs modified Au electrode. Cyclic voltammograms of DNA–AuNPs showed no peak current in the potential range from −0.6 V to 0.2 V vs SCE (Fig. 4, curve b). Comparing with the DNA–AuNPs, FeTMPyP–DNA–AuNPs modified

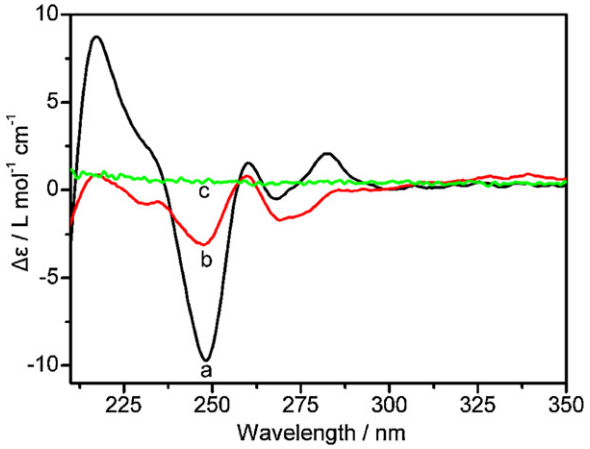

Fig. 2. CD spectra of dsDNA (a), FeTMPyP–dsDNA (b) and FeTMPyP (c).

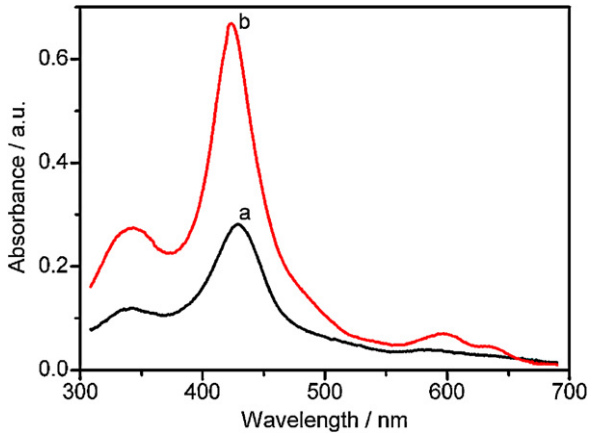

Fig. 3. UV–vis spectra of FeTMPyP–dsDNA (a) and FeTMPyP (b).

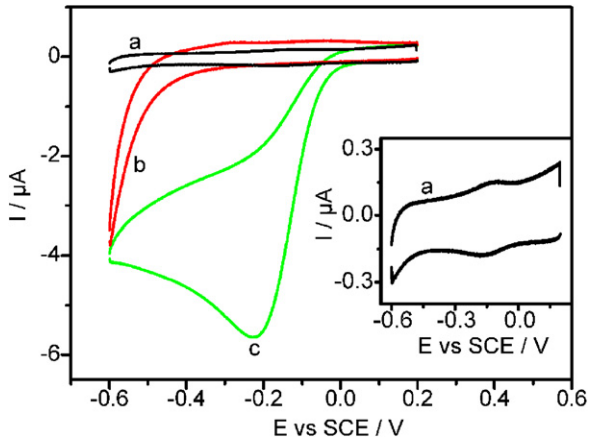

Fig. 4. Cyclic voltammograms of FeTMPyP–DNA–AuNPs probe on gold electrode in N_2-saturated (a) and O_2-saturated (c) Tris–HCl buffer, and (b) is cyclic voltammogram of DNA–AuNPs in O_2-saturated Tris–HCl buffer. Inset: amplification of curve a. Scan rate: 100 mV s^{-1}.

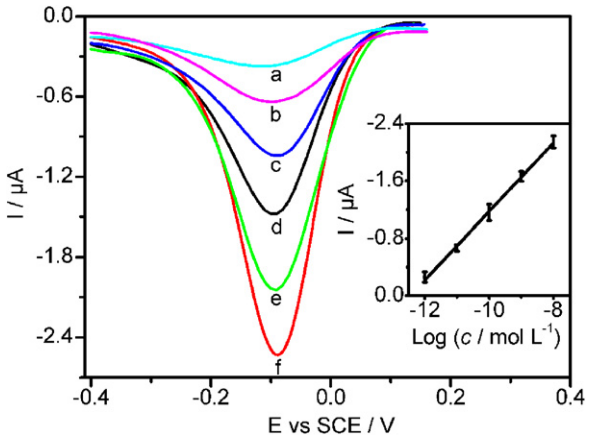

Fig. 6. DPV curves at target concentrations of 0 (a), 1×10^{-12} (b), 1×10^{-11} (c), 1×10^{-10} (d), 1×10^{-9} (e) and 1×10^{-8} (f) mol L^{-1}. Inset: linear relationship between peak current and the logarithm of target DNA concentration.

Au electrode has a large response at −0.228 V vs SCE (Fig. 4, curve c), which suggested that FeTMPyP has the excellent electrocatalysis to O_2 reduction. The possible mechanism is that $Fe^{(III)}$TMPyP was firstly reduced to $Fe^{(II)}$TMPyP at electrode surface, followed by binding with O_2 to form the ferrous-peroxo intermediate, and at a more negative potential the complex was further reduced to give the product and release $Fe^{(II)}$TMPyP [13]. Moreover, the probe was stable enough to maintain its catalytic activity even for a month and 94.3% of the signal was still observed, suggesting the structure of FeTMPyP–DNA–AuNPs modified electrode was efficient for retaining the activity of FeTMPyP and preventing it from leaking out of the biosensor. Based on the enhanced current, a sensitive and stable biosensor should be constructed for the detection of target DNA.

3.3. Optimization of fabrication of the probe

In order to obtain the enhanced sensitivity, the molar ratio of [FeTMPyP]/[dsDNA] was investigated. Fig. 5 shows the CD spectra of dsDNA at the different molar ratio of [FeTMPyP]/[dsDNA]. When the molar ratio of [FeTMPyP]/[dsDNA] is 0 (curve a), dsDNA exhibited characteristic bands at 217 nm and a 'double peak' around 275 nm. Upon addition of FeTMPyP, the intensities of band at 217 nm decrease (curves b and c), which indicating that FeTMPyP has bound to the dsDNA and diminished the dA stacking [37]. When the ratio measured up to 30 (curve d), no obvious CD signal could be observed, which may be attributed to that DNA-binding sites were all occupied by FeTMPyP and minimized dA stacks within the strand. So the molar ratio of 30 is enough for loading of FeTMPyP during the preparation of the detection probe.

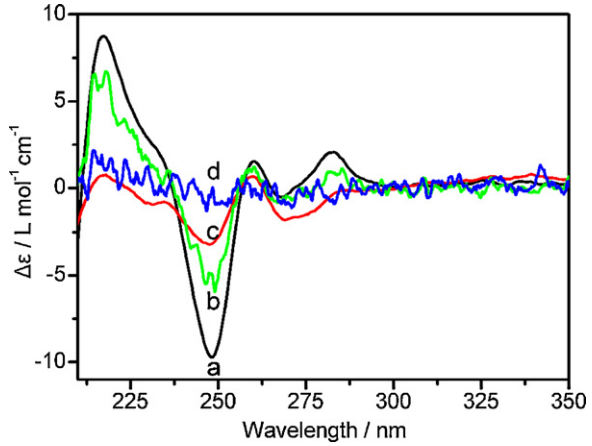

Fig. 5. CD spectra of FeTMPyP–dsDNA at the molar ratio of [FeTMPyP]/[dsDNA] of 0 (a), 4 (b), 20 (c) and 30 (d).

3.4. Amperometric sensing of target DNA

Under the optimal conditions, the sensitivity of our detection strategy was investigated by varying the target DNA concentration. Fig. 6 shows typical DPV curves of the sensor with the target DNA at different concentration. The blank should derivate from the nonspecific adsorption of FeTMPyP–DNA–AuNPs probe on the electrode (Fig. 6, curve a). The response was logarithmically related to the target concentration across a range of 1×10^{-12} to 1×10^{-8} mol L^{-1} with a detection limit of 2.5×10^{-13} mol L^{-1} at a signal-to-noise ratio of 3 (Fig. 6, inset). The regression equation was $I = -5.94 - 0.48 \times \log c$ with a correlation coefficient of 0.9993, where I is the peak current of the biosensor, and c is the concentration of target DNA. The detectable concentration range of 4 orders of magnitude was relatively wide. This high sensitivity highlighted the importance of using DNA–AuNPs to carry numerous FeTMPyP and significantly amplified the current based on the bionic catalysis.

Selectivity is also an important parameter for a biosensor. The specificity of the proposed DNA biosensor was investigated by exposing it to three kinds of DNA sequences, including perfect complementary target, single-base mismatched oligonucleotide and three-base of mismatched oligonucleotide at the same concentration (1×10^{-9} mol L^{-1}). As shown in Fig. 7, the biosensor

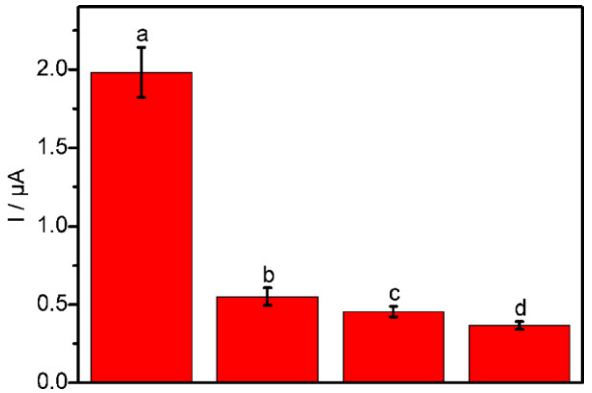

Fig. 7. Histograms of peak currents for complementary sequence (a), single-base mismatched sequence (b), three-base mismatched sequence (c) and blank (d).

presented good performance to discriminate complementary target and the bases mismatched oligonucleotides. The signals of single-base mismatched oligonucleotide and three-base of mismatched oligonucleotide are 3.7 and 4.5 times lower than that of target DNA, respectively, and are closed to the response of blank. These results demonstrated that the proposed approach was able to effectively detect the target with specificity. The reproducibility of the biosensor was examined at the same modified electrode. The relative standard deviation for six measurements was 2.7%, thus giving good intra-reproducibility. In addition, the relative standard deviation of signals for measurement of 1×10^{-9} mol L^{-1} target at six independently prepared biosensors was 3.1%, which proved good reproducibility of the biosensor preparation.

4. Conclusions

A novel electrochemical strategy was developed for the detection of DNA based on the bionic catalysis of porphyrin. The detection probe of porphyrin–DNA–AuNPs was successfully prepared via groove binding between FeTMPyP and DNA–AuNPs along the dsDNA surface, leading to a densely FeTMPyP on the DNA–AuNPs. The FeTMPyP–DNA–AuNPs probe on gold electrode demonstrated the excellent electrocatalytic behaviors toward the reduction of O_2, since both AuNPs and DNA accelerated the electron transfer between FeTMPyP and the electrode, and increased the amount of adsorbed FeTMPyP. Based on bionic catalysis of porphyrin, the resulting biosensor exhibited a good performance for the detection of DNA with a 4-order wide linear range, effective discrimination to specific target, and acceptance fabrication reproducibility. Moreover, the advantage of the biosensor was that the whole experiment is carried out without oxygen removal. This strategy based on bionic catalysis of porphyrin as detection probe provides a new concept for the development of analytical method, and could be conveniently extended for sensitive detection of other important biomolecules.

Acknowledgements

This research was financially supported by the National Natural Science Foundation of China (21135002, 21075060, 21121091, 20835006), the Program for New Century Excellent Talents in University (NCET100479), and Science Foundation of Jiangsu (BK2010302).

References

[1] J. Huang, Y.R. Wu, Y. Chen, Z. Zhu, X.H. Yang, C.Y.J. Yang, K.M. Wang, W.H. Tan, Angewandte Chemie International Edition 50 (2011) 401.
[2] H.F. Dong, W.C. Gao, F. Yan, H.X. Ji, H.X. Ju, Analytical Chemistry 82 (2010) 5511.
[3] G.J. Li, L.H. Liu, X.W. Qi, Y.Q. Guo, W. Sun, X.L. Li, Electrochimica Acta 63 (2012) 312.
[4] G. Liu, Y. Wan, V. Gau, J. Zhang, L.H. Wang, S.P. Song, C.H. Fan, Journal of the American Chemical Society 130 (2008) 6820.
[5] X.D. Su, H.F. Teh, X.H. Lieu, Z.Q. Gao, Analytical Chemistry 79 (2007) 7192.
[6] H.F. Dong, Z. Zhu, H.X. Ju, F. Yan, Biosensors and Bioelectronics 33 (2012) 228.
[7] H.Q. Wang, W.Y. Liu, Z. Wu, L.J. Tang, X.M. Xu, R.Q. Yu, J.H. Jiang, Analytical Chemistry 83 (2011) 1883.
[8] R.Z. Fu, T.H. Li, S.S. Lee, H.G. Park, Analytical Chemistry 83 (2011) 494.
[9] C.Y. Yean, B. Kamarudin, D.A. Ozkan, L.S. Yin, P. Lalitha, A. Ismail, M. Ozsoz, M. Ravichandran, Analytical Chemistry 80 (2008) 2774.
[10] J. Li, S.P. Song, X.F. Liu, L.H. Wang, D. Pan, Q. Huang, Y. Zhao, C.H. Fan, Advanced Materials 20 (2008) 497.
[11] W.C. Gao, H.F. Dong, J.P. Lei, H.X. Ji, H.X. Ju, Chemical Communications 47 (2011) 5220.
[12] A. Singh, S. Patra, J. Lee, K.H. Park, H. Yang, Biosensors and Bioelectronics 26 (2011) 4798.
[13] J.P. Collman, R. Boulatov, C.J. Sunderland, L. Fu, Chemical Reviews 104 (2004) 561.
[14] X. Xu, H.J. Lu, J.V. Ruppel, X. Cui, S.L.D. Mesa, L. Wojtas, X.P. Zhang, Journal of the American Chemical Society 133 (2011) 15292.
[15] Z.Q. Cong, T. Kurahashi, H. Fujii, Journal of the American Chemical Society 134 (2012) 4469.
[16] W.M. Ching, C.H. Chuang, C.W. Wu, C.H. Peng, C.H. Hung, Journal of the American Chemical Society 131 (2009) 7952.
[17] I. Yamanaka, T. Onizawa, H. Suzuki, N. Hanaizumi, N. Nishimura, S. Takenaka, Journal of Physical Chemistry C 116 (2012) 4572.
[18] T.P. Umile, D. Wang, J.T. Groves, Inorganic Chemistry 50 (2011) 10353.
[19] J. Heinecke, P.C. Ford, Coordination Chemistry Reviews 254 (2010) 235.
[20] L.E. Goodrich, F. Paulat, V.K.K. Praneeth, N. Lehnert, Inorganic Chemistry 49 (2010) 6293.
[21] X.Q. Lu, F.P. Zhi, H. Shang, X.Y. Wang, Z.H. Xue, Electrochimica Acta 55 (2010) 3634.
[22] A. Okunola, B. Kowalewska, M. Bron, P.J. Kulesza, W. Schuhmann, Electrochimica Acta 54 (2009) 1954.
[23] J.X. Geng, H.T. Jung, Journal of Physical Chemistry C 114 (2010) 8227.
[24] J. Li, W.W. Tu, J.P. Lei, S. Tang, H.X. Ju, Electrochimica Acta 56 (2011) 3159.
[25] W.W. Tu, J.P. Lei, H.X. Ju, Chemistry – A European Journal 15 (2009) 779.
[26] W.W. Tu, J.P. Lei, G.Q. Jian, Z. Hu, H.X. Ju, Chemistry – A European Journal 16 (2010) 4120.
[27] W.W. Tu, J.P. Lei, S.Y. Zhang, H.X. Ju, Chemistry – A European Journal 16 (2010) 10771.
[28] R.J. Fiel, J.C. Howard, E.H. Mark, N.D. Gupta, Nucleic Acids Research 6 (1979) 3093.
[29] G. Ananyan, A. Avetisyan, L. Aloyan, Y. Dalyan, Biophysical Chemistry 156 (2011) 96.
[30] S. Lee, S.H. Jeon, B.J. Kim, S.W. Han, H.G. Jang, S.K. Kim, Biophysical Chemistry 92 (2001) 35.
[31] R.F. Pasternack, E.J. Gibbs, J.J. Villafranca, Biochemistry 22 (1983) 2406.
[32] P. Kara, D. Ozkan, K. Kerman, B. Meric, A. Erdem, M. Ozsoz, Analytical and Bioanalytical Chemistry 373 (2002) 710.
[33] A. Ambrosi, M.T. Castañeda, A.J. Killard, M.R. Smyth, S. Alegret, A. Merkoçi, Analytical Chemistry 79 (2007) 5232.
[34] Z.Q. Zhu, Y.Y. Su, J. Li, D. Li, J. Zhang, S.P. Song, Y. Zhao, G.X. Li, C.H. Fan, Analytical Chemistry 81 (2009) 7660.
[35] Y. Jin, W. Lu, J.Q. Hu, X. Yao, J.H. Li, Electrochemistry Communications 9 (2007) 1086.
[36] J.S. Wang, L. Wu, J.S. Ren, X.G. Qu, Small 8 (2012) 259.
[37] N.K. Schwalb, F. Temps, Science 322 (2008) 243.
[38] A.M. Brun, A. Harriman, Journal of the American Chemical Society 116 (1994) 10383.
[39] Q. Zhao, Z.N. Gu, Q.K. Zhuang, Electrochemistry Communications 6 (2004) 83.